Thermal and optical properties of tellurite glasses doped erbium

I. Jlassi · H. Elhouichet · M. Ferid

Abstract Er^{3+}-doped tellurite glasses with molar compositions of $75TeO_2$–$20ZnO$–$(5 - x)$ Na_2O–xEr_2O_3 ($x = 0$, 0.5, 1, 2, 3, and 4 mol%) have been elaborated from the melt-quenching method. The effects of Er_2O_3 concentration on the thermal stability and optical properties of tellurite glasses have been discussed. From the differential scanning calorimetry (DSC) profile, the glass transition temperature T_g, and crystallization onset temperature T_x are estimated. The thermal stability factor, defined as $\Delta T = T_x - T_g$, was higher than 100 °C. It suggests that tellurite glass exhibits a good thermal stability and consequently is suitable to be a potential candidate for fiber drawing. Furthermore, the stability factor increases with Er_2O_3 concentration up to 2 mol% then presents a continue decrease suggesting of beginning of crystallization of highly doped tellurite glasses. The refractive index and extinction coefficient data were obtained by analyzing the experimental spectra of $\tan\Psi$ and $\cos\Delta$ measured by spectroscopic ellipsometry (SE). The complex dielectric functions ($\varepsilon = \varepsilon_1 + i\varepsilon_2$) of the samples were estimated from regression analysis. The fundamental absorption edge has been identified from the optical absorption spectra and was analyzed in terms of the theory proposed by Davis and Mott. The values of optical band gap for direct and indirect allowed transitions have been determined. An important decrease of the optical band gap was found after Er doping. It was assigned to structural changes induced from the formation of non-bridging oxygen. The absorption coefficient just below the absorption edge varies exponentially with photon energy indicating the presence of Urbach's tail. The origin of the Urbach energy is associated with the phonon-assisted indirect transitions.

Introduction

The use of optical waveguide and laser allows exploitation of materials with smaller nonlinear index coefficients, ideally, materials with a high damage threshold and a large region of high transparency. In recent years, the rare earth (RE) doped optical materials have been extensively investigated due to their potential applications in many fields, such as color display, optical data storage, sensor, laser, and optical amplifier for communication [1–5]. Er^{3+}-doped fiber amplifier (EDFA) is one of the key devices for use in 1.5 μm wavelength optical communication window. Among these materials, particular attention has been devoted to the study of tellurite glasses. Tellurite glasses have been extensively investigated, mainly due to their interesting physical properties, but also from a fundamental point of view. Their unusually large infrared transparency, high linear and non-linear refractive indices, good thermal stability and corrosion resistance and suitability as a matrix for active element doping, represent the main justification for their continuous technological interest [6], which could be a good candidate for fiber drawing [7]. Tellurite glasses are widely used as photonic crystal fibers (PCFs) and also Er-doped Na_2O–ZnO–TeO_2 glasses are known and being studied earlier also [8, 9]. TeO_2 glasses are known to be low melting and high refractive index materials, therefore considered to be potential nonlinear materials (therefore the PCFs, for example) [10]. They show potential applications

I. Jlassi (✉) · H. Elhouichet · M. Ferid
Laboratoire de Physico-Chimie des Matériaux Minéraux et leurs Applications, Centre National de Recherches en Sciences des Matériaux, B.P. 95, Hammam-Lif 2050, Tunisia
e-mail: ifa.jlassi@fst.rnu.tn

H. Elhouichet
Département de Physique, Faculté des Sciences de Tunis, Campus ElManar 2092, Tunisia

in third-order non-linear optics (NLO) as well, due to the unique refractive dispersion nature [11].

These good properties of tellurite glasses need to be optimized versus the molar concentration of the doping RE elements. We assume that a systematic study of both thermal and optical properties of tellurite glasses with Er_2O_3 concentration, for example, may facilitate the acquaintance of the fundamental characteristics of the glass and to optimize both the thermal stability and quantum efficiency. The optical properties of tellurite glasses doped with RE have been investigated by several groups [12–15]. In fact, the determination of optical parameters such as refractive index, extinction coefficient, band gap energy, material dispersion of these glasses, and their nonlinear aspects is a topic of fundamental and technological importance. Optical absorption in solids occurs by various mechanisms, in all of which the photon energy will be absorbed by either the lattice or by electrons where the transferred energy is covered. It is a useful method for optical investigation of induced transitions and for getting information about the band structure and energy gap of non-crystalline materials. The study of variation of optical band gap with Er_2O_3 composition gives information regarding the structure and the nature of bonds in the matrix.

This work analysis the thermal stability and optical properties of TeO_2–ZnO–Na_2O (TZN) glass doped with different concentration of Er^{3+}. The thermal stability factor is determined from differential scanning calorimetry (DSC) profile. The refractive index and the extinction coefficient of the present glasses are determined using spectroscopic ellipsometry (SE) measurements. Analysis of absorption edge yields both direct and indirect allowed transitions with their optical energy gaps and given up the Urbach energy as well.

Experimental details

Sample preparation

Glasses with compositions of $75TeO_2$–$20ZnO$–$(5 - x)$ Na_2O–xEr_2O_3 ($x = 0$, 0.5, 1, 2, 3, and 4 mol%) (referred TZNEr) were prepared by melt quenching. Reagent grade commercial oxides ($\sim$99.99% purity, Aldrich) were used as the starting materials. The mixed oxides were melted in platinum crucibles at 850 °C for $\sim$1 h. Then, the glass liquid was poured into a stainless mold. Immediately after the quench, the glass (as-prepared sample) was annealed at 250 °C (for 1 h) and then slowly cooled until ambient temperature. The annealing process sought to minimize the internal mechanical stress and obtain glasses with good mechanical stability. The choice of annealing at 250 °C was based on the knowledge of behavior of other glasses with

similar compositions, whose heat treatment at 250 °C was enough to decrease/eliminate the internal tensions [16]. The result was a colorless glass with good mechanical stability. The obtained glasses were cut and polished carefully in order to meet the requirements for optical measurements.

Optical and spectroscopic measurements

UV/Vis/NIR absorption spectra for all Er^{3+}-doped samples were obtained at room temperature (RT) using a Varian 5000 spectrometer in the range of 200–1700 nm. Small pieces of glass were used to measure the glass transition temperature T_g and crystallization onset temperature T_x by means of DSC Metler Toldo DSC823^e at a heating rate of 10 °C/min from RT to 700 °C using an aluminum oxide ceramic pan.

SE measurements were performed using an automatic ellipsometer SOPRA GES5. The system uses a 75 W xenon lamp, a rotating polarizer, an autotracking analyzer, a double monochromator, and as detectors: a photomultiplier detector and a AlGaAs:P photodiode. Data were collected in the 1.0–5.0 eV photon energy region with the resolution of 10 meV, at an incidence angle $\Phi_0 = 73°$. All the optical measurements were carried out at RT.

Results and discussion

Thermal properties

From DSC curve (Fig. 1) characteristic temperatures such as glass transition temperature T_g, crystallization onset T_x, and maximum of the crystallization peak T_p were obtained, from which stability factor $\Delta T = T_x - T_g$, was calculated.
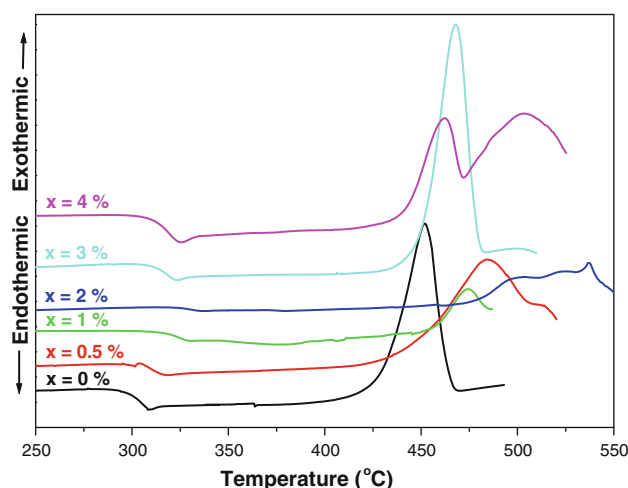

Fig. 1 DSC scans of TZNEr glass system with various Er^{3+} content

The stability of the tellurite glasses was also analyzed using the Hruby [17] parameter as follows:

$$H = \frac{(T_x - T_g)}{T_g} \qquad (1)$$

H was used to express and evaluate the stability of the glass against crystallization. Hruby's parameter is well known in the sense that it evaluates glass forming ability. The larger the H, the better the glass forming ability. The results of thermal parameters, for different Er^{3+} concentrations, are presented in Table 1.

From Table 1, we can deduce that a stable and wide glass formation range may be obtained. The selection of good glass compositions can be made on the basis of thermal stability parameter, which is one of the most important factors for fiber drawing. The difference ΔT has frequently been used as a rough estimate of the glass formation ability or glass stability, since fiber drawing is a reheating process and any crystallization in the process will increase the scattering loss of the fiber and then degrade the optical properties [18]. To achieve a large working range of temperature during the sample fiber drawing, it is desirable for a glass host to have ΔT as large as possible [19]. According to literature [20], if the value of ΔT is higher than 100 °C, the glass can be considered as thermally stable. For all Er_2O_3 concentrations studied in this work, the thermal stability factor is higher than 100 °C (Table 1), which suggests that it is suitable for a potential application in fiber drawing. The data in Table 1 imply that an optimum doping level with Er^{3+} does exist (at about 2 mol% Er_2O_3) at which thermal stability of the glass is optimized. The increase of ΔT mostly resulted from the increase of T_x. Further doping the glass up to 2 mol% shows a continuous decrease of ΔT which reflects the decrease of thermal stability. For TZN doped 4 mol% of Er_2O_3, the DSC curve shows the existence of second exothermic peak which indicates that partial crystallization can takes place in the glass. In the same context, Tikhomirov et al. [21] show that TZN glasses have good thermal stability for low Er concentration. However, for relatively high Er^{3+} concentrations (up to 4 mol%) TZN have poor thermal stability and tend to crystallization. In comparison with other glasses, the optimized value of ΔT (case of 2 mol%) is larger than that of oxychloride tellurite glasses (120 °C) [22], gadolinium borosilicate glasses (130 °C) [23], barium gallo-germanate glass (131 °C) [24], oxyfluoro-tellurite glasses (140 °C) [25], germanate–borate glasses (138 °C) [26], and fluoride glasses (105 °C) [27–29].

Ellipsometry measurements

SE has been applied to assess optical constants of samples. It provides information on the optical properties (index of refraction n and extinction coefficient k) of materials by reflecting monochromatic polarized light off of a sample and examining the change in the polarization of the light caused by the reflection. In this work, ellipsometric measurements were performed at an angle of incidence $\Phi_0 = 73°$ in the photon energy $h\nu$ range 1–5 eV.

The measured quantity is the complex reflectance ratio ρ defined by:

$$\rho = \frac{r_p}{r_s} = \tan\Psi \exp(i\Delta) \qquad (2)$$

where r_p and r_s are the complex-valued reflection coefficients for light polarized parallel (index p) and perpendicular (index s) to the plane of incidence, respectively. Ψ and Δ are called the ellipsometric angles and are often said to be the experimentally determined quantities obtained from an ellipsometer.

Figure 2 shows the ellipsometric spectra of $\tan\Psi$ and $\cos\Delta$ of TZNEr glasses (case of 2 mol% as example) in the UV–Vis–IR range. The same appearance given on Fig. 2 was observed for all concentration Er^{3+} studied.

One basic quantity to determine is the complex refractive index $N = n + ik$ of the sample.

Table 1 Thermal parameters of Er-doped tellurite glass

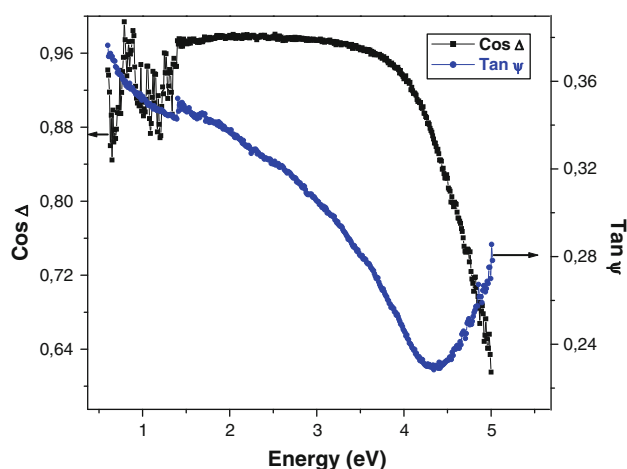| Er^{3+} content (mol%)	T_g (°C)	T_x (°C)	T_p (°C)	ΔT (°C)	H
$x = 0$	299	429	451	130	0.43
$x = 0.5$	305	442	484	137	0.44
$x = 1$	316	456	474	140	0.44
$x = 2$	319	478	537	159	0.49
$x = 3$	310	450	468	140	0.45
$x = 4$	309	442	462	133	0.43

Fig. 2 Spectra of $\tan\Psi$ and $\cos\Delta$ for TZNEr glasses, case of $x = 2$ mol% is given as an example
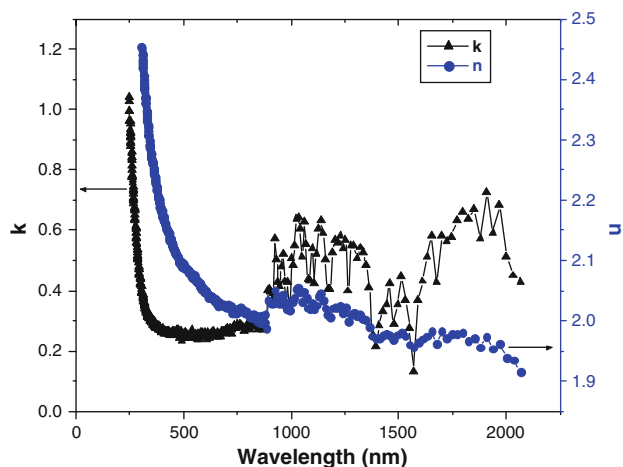
Fig. 3 Refractive index $n(\lambda)$ and extinction coefficient $k(\lambda)$ of TZNEr glasses (case of $x = 2$)

From the measured ρ, $\langle N \rangle$ was determined using [30]:

$$\langle N \rangle = \sin \Phi_0 \sqrt{1 + (\frac{1-\rho}{1+\rho})^2 \tan^2 \Phi_0} \quad (3)$$

Figure 3 shows the data of both the refractive index n and extinction coefficient k of TZNEr (case of 2 mol% as example) in the UV–Vis–IR range. TZNEr glasses have large refractive indices and obvious dispersion. n and k show a slight variation in the visible and IR ranges. However, because of the high absorption of glasses in the UV range, both the values of n and k are important.

One of the basic parameter that characterizes a given glass as an optical material is the refractive index dispersion or the material dispersion [31]. For an instant, refractive index dispersion is of major importance in fiber optic telecommunications [32–34] to attain maximum information capacity in single-mode glass fiber. The dispersion measurements are very important when one is looking for nonlinear material characterization, especially if the incident wavelength of the pump beam is around the band gap when the linear absorption cannot be neglected.

These refractive indices have been used in evaluating the Cauchy's constants (A, B, and C). The Cauchy's formula of refractive index n, as a function of the wavelength λ, is given by:

$$n = A + \frac{B}{\lambda^2} + \frac{C}{\lambda^4} \quad (4)$$

The computed values of the Cauchy's constants are determined by fitting the curve of $n(\lambda)$ (Table 2). However, in the transparency region of the material, the coefficient C is very small so it can be ignored.

The complex dielectric is as follow: $\varepsilon(\lambda) = \varepsilon_1(\lambda) + i\varepsilon_2(\lambda) = N^2$. The real part ε_1 and the imaginary part ε_2 are given as:

Table 2 Cauchy coefficients (A, B), optical band gap for direct (E_{opt}^{dir}) and indirect (E_{opt}^{ind}) transitions and Urbach (E_U) energy of TZNEr glasses

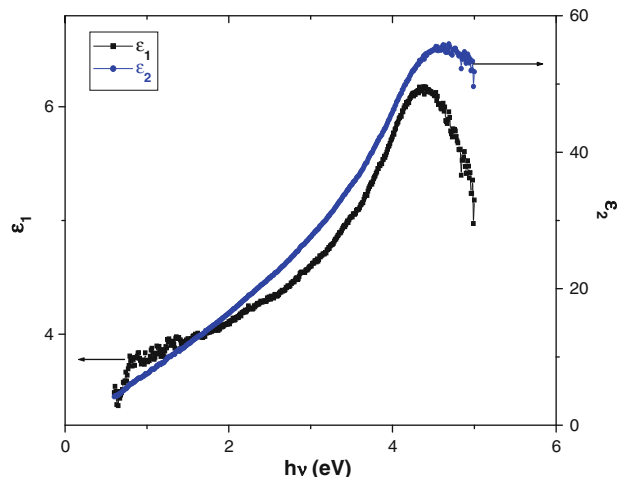| Er_2O_3 (mol%)	0	0.5	1	2	3	4
A	2.01	2.002	1.99	1.998	1.997	1.970
B (nm^2) $\times 10^3$	11.134	12.186	13.785	14.931	15.973	16.202
E_{opt}^{ind} (eV) (± 0.01)	3.626	3.234	3.232	3.230	3.215	3.223
E_{opt}^{dir} (eV) (± 0.01)	3.347	3.201	3.171	3.196	3.143	3.167
E_U (eV) (± 0.001)	0.221	0.113	0.181	0.107	0.14	0.186

Fig. 4 Real and imaginary part of dielectric constant, versus photon energy, of the TZNEr glass (case of $x = 2$)

$$\varepsilon_1 = n^2 - k^2 \quad (5)$$

$$\varepsilon_2 = 2nk \quad (6)$$

For all samples, Fig. 4 shows that the dielectric constant has an exponential steady increase with photon energy. This means that the free carrier concentration (assuming that the free carrier effective mass is a constant in the first approximation) of the different glass compositions changes in the same manner with the change in Er_2O_3 content. The determination of the imaginary part ε_2 could be employed in the determination of the optical relaxation time of glasses. Similar variations of both ε_1 and ε_2 are observed for the others Er_2O_3 molar concentrations in TZNEr.

Optic band gap

The measurement of optical absorption and the absorption edge is important especially in connection with the theory of electronic structure of amorphous materials. The study of the optical absorption edge in UV-region has proved to be a very useful method for elucidation of optical transitions and electronic band structure of materials [35]. It is
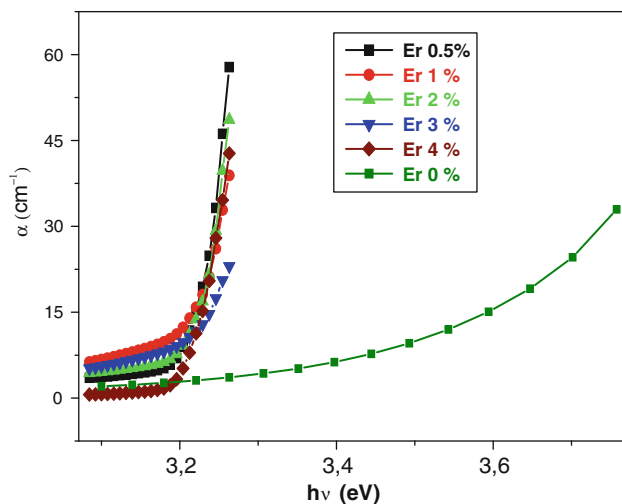
Fig. 5 Optical absorption as a function of photon energy for the TZNEr glass system

possible to determine indirect and direct transition occurring in band gap by optical absorption spectra at the fundamental absorption edge of the material.

The optical absorption spectra for Er^{3+}-doped tellurite glasses, in the UV range, are shown in Fig. 5. The absorption coefficient α can be written as [36]:

$$\alpha = \frac{1}{d}\ln\left(\frac{I_0}{I}\right) \tag{7}$$

where d is the thickness of the sample, $\ln\left(\frac{I_0}{I}\right)$ corresponds to absorbance.

Figure 5 shows that the optical absorption edge is not sharply defined in the TZNEr glasses, in accordance with their amorphous nature.

Davis and Mott [36] gave an expression for the absorption coefficient, $\alpha(v)$, as function of photon energy (hv) for direct and indirect optical transitions:

$$\alpha(v) = \frac{A(hv - E_{opt})^n}{hv} \tag{8}$$

where A is an energy-independent constant, E_{opt} is the optical band gap and n is a constant which determines type of the optical transition. $n = 2$ corresponds to indirect allowed transition and $n = \frac{1}{2}$ corresponds to direct allowed transition. The optical data are analyzed for the higher values of $\alpha(v)$ above the exponential region. Figure 6 represents the variation of $(\alpha hv)^{1/2}$ and $(\alpha hv)^2$ as a function of photon energy (hv) for direct and indirect transitions, respectively case of 2 mol% Er_2O_3 is taken as example. The E_{opt} values with an accuracy of ± 0.01 eV obtained by extrapolation to $(\alpha hv)^{1/2} = 0$ and $(\alpha hv)^2 = 0$ for direct and indirect allowed transitions, respectively. Optical band gap values for indirect (E_{opt}^{ind}) and for direct (E_{opt}^{dir}) allowed transitions in Er^{3+}-doped TZNEr glasses are given in Table 2. Particular interest can be devoted to the optical
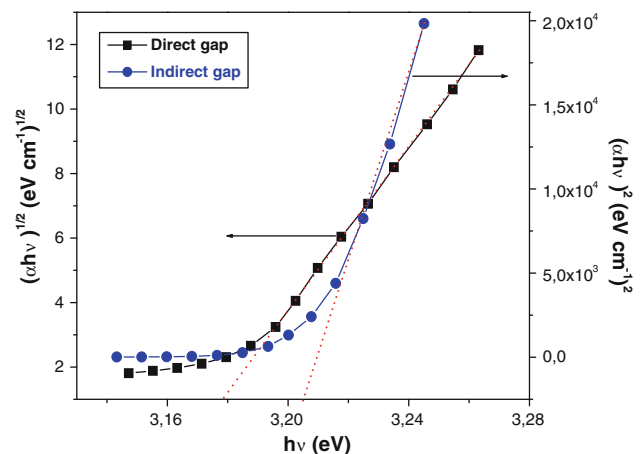

Fig. 6 Determination of the optical energy band gap for direct (E_{opt}^{dir}) and indirect (E_{opt}^{ind}) transition in TZNEr glasses (case of $x = 2$)

band gap of non-doped glass. Its value show that TZN glass has direct band gap since E_{opt}^{ind} exceeds E_{opt}^{dir} by ≈ 0.28 eV. Furthermore, for all the Er_2O_3 composition in TZNEr glasses, the value of E_{opt}^{dir} is slightly less than that of E_{opt}^{ind} which indicate that the allowed transition in TZN glass keep the same after introduction of Er. The main remark that can be shown from Table 2 is the relatively important decrease of the band gap after Er doping since for non-doped TZN glass, E_{opt}^{dir} decreases by 0.14 eV after doping with 0.5 mol% of Er_2O_3. However, for TZNEr glass, E_{opt} is weakly sensitive to Er_2O_3 composition.

The reduction of the band gap after Er doping is attributed to the structural changes that are taking place in the glass with incorporation of Er_2O_3. It is known that the changes induced in glass structure as a result of the introduction of RE ions include the formation of greater number of non-bridging oxygens (NBOs) [37] which accordingly decreases E_{opt}. It is generally accepted that the location of absorption edge depends on the oxygen bond strength in the glass forming network [38]. The introduction of RE changes the oxygen bonding in glass forming network and any change of oxygen bonding in glass network such as the formation of NBO changes the absorption characteristics. On other hand, when one molecule of Er_2O_3 is introduced into the tellurite matrix, coordination number of Te atoms changes. As the concentration of Er_2O_3 reaches greater than 0.5 mol%, NBOs would start to form. It is well reported that at low concentration, Er_2O_3 acts as network modifier in place of network former. Optical band gap is influenced not only by a chemical composition but also by a structural arrangement of the sample matrix. It has been shown from ab initio molecular orbital calculations that the difference between Homo- and Lumo-state is low for TeO_4 unit whereas it is high for TeO_3 [39] and even for TeO_{3+1} units [40]. It means that broader optical band gap can be observed for TeO_2

based glasses if the density of TeO_3 and/or TeO_{3+1} unit assists significantly to the network formation. However, these changes are not sufficient to account for the observed decrease in the optical band gap. With the substitution of ZnO oxides into TeO_2, bridging Te–O–Te bonds are broken and non-bridging Te–O–Zn^{2+} bonds are formed. The NBO bonds have a much greater ionic character and much lower bond energies. Consequently, the NBO bonds have higher polarizability and cation refractions.

Determination of Urbach energy

The main feature of the absorption edge of amorphous materials is an exponential increase of the absorption coefficient with photon energy. When the energy of the incident photon is less than the band gap, the increase in absorption coefficient is followed with an exponential decay of density of states localized into the gap [41]. The absorption edge here is called Urbach edge, where the obtained values are between 10 and 10^3 cm^{-1}. The lack of crystalline long-range order in amorphous/glassy materials is associated with a tailing of density of states into normally forbidden energy [41]. The band tail associated with valence band and conduction band, which is developed due to the potential fluctuations in the material, extends into the energy gap and normally shows an exponential behavior. Urbach energy characterizes the extent of the exponential tail of the absorption edge. The exponential absorption tails and Urbach energy is given in accordance with the empirical relation [42]:

$$\alpha(\upsilon) = \alpha_0 \exp(\frac{h\upsilon}{E_U}) \qquad (9)$$

where α_o is a constant, E_U is the Urbach energy which indicates the width of the band tails of the localized states and υ is the frequency of the radiation.

The main factor contributing to edge broadening in crystalline materials is exciton–phonon coupling (dynamic disorder). In amorphous materials, an additional broadening, due to static disorder, exists.

Experimentally, plots [43] are drawn for ln(α) against photon energy, $E = h\upsilon$, case of 2 mol% Er_2O_3 is taken as example (Fig. 7). The Urbach energy is calculated by taking the reciprocals of the slopes of the linear portion in the lower photon energy of these curves. From Table 2 it can be seen that the Urbach energy of these glasses does not admit a linear aspect by varying the Er content. The E_U values are determined for the present glasses and found to lie between 0.107 and 0.221 eV. The origin of this ΔE can be considered as the cluster of the localized states below the conduction band. These phonons assist the indirect transitions of the electrons to the conduction band and account for the observed fundamental absorption edge of
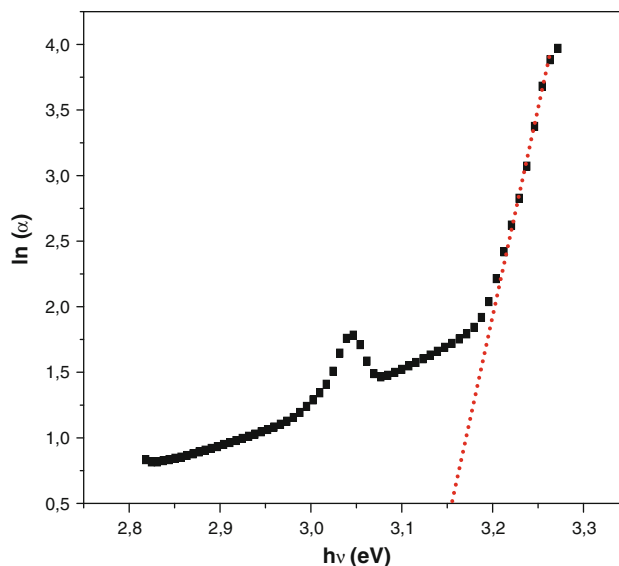

Fig. 7 Logarithm of the absorption coefficient, ln(α), against photon energy, $h\upsilon$, to obtain Urbach energy of TZNEr glasses (case of $x = 2$)

the TZNEr glass. It is generally assumed that the exponential tail observed in various materials must have the same physical origin and this origin can be attributed to the phonon-assisted indirect electronic transitions [44, 45]. The obtained results are in accordance with those reported for inorganic glasses [46].

Conclusion

In this work, the thermal and optical properties of TZNEr glasses have been investigated. From DSC measurements, we have determined the glass transition temperature T_g and crystallization onset temperature T_x. The thermal stability factor $\Delta T = T_x - T_g$ was found higher than 100 °C, which suggests that tellurite glass is thermally stable. The DSC result suggests that TZNEr glass is suitable for a potential application in fiber drawing. The optical constants and other dispersion parameters of the studied glasses are determined in a wide spectral range. The evaluated refractive indices indicate that the glass becomes optically more dispersive and the refractive index can be tuned depending on the amount of Er_2O_3 present on the glass matrix. Analysis of absorption edges yields both direct and indirect allowed transitions with their optical energy gaps. The Urbach energy is determined from the band tail absorption. The studied TZNEr system shows the direct and indirect optical band gap in the range from 3.143 to 3.347 eV and 3.215 to 3.626 eV respectively. The values of Urbach energy confirm the existence of phonon-assisted transitions.

References

1. Wang JS, Vogel EM, Snitzer E (1994) Opt Mater 3(3):187
2. Chen D et al (2007) J Appl Phys 101(11):113511
3. Kishi Y et al (2005) J Am Ceram Soc 88(12):3423
4. Tanabe S et al (2002) Opt Mater 19(3):343
5. Liu YH et al (2007) J Opt Soc Am B 24(5):1046
6. El-Mallawany RAH (2001) Tellurite glasses handbook-physical properties and data. CRC, Boca Raton, FL
7. Jewell JM, Busse LE, Crahan K, Harbison BB, Aggarwal ID (1994) Proc SPIE 2287:154
8. Souza Neto NM, Ramos AY, Barbosa LC (2002) J Non-Cryst Solids 304:195
9. Jha A, Shen S, Naftaly M (2000) Phys Rev B 62:6215
10. Ravi Kanth Kumar VV, George AK, Knight JC, Russell PSJ (2003) Opt Exp 11:2641
11. Vijaya Prakash G, Narayana Rao D, Bhatnagar AK (2001) Solid State Commun 119:39
12. Wang JS, Vogel EM, Snitzer S (1994) Opt Mater 3:187
13. Xu S, Fang D, Zhang Z, Jiang Z (2005) J Solid State Chem 178:1817
14. Ryba-Romanwski W, Golab S, Cichosz L, Jezowaska-Trzebiatawska B (1988) J Non-Cryst Solids 105:295
15. Biswal S, Nees J, Nishimura A, Takuma H, Mourou G (1999) Opt Commun 160:92
16. Graça MPF, Ferreira da Silva MG, Valente MA (2008) J Non-Cryst Solids 354:901
17. Hruby H (1972) Czech J Phys B 32:1187
18. Xu SQ, Yang ZM, Dai SX, Yang JH (2003) Chin Phys Lett 20:905
19. Neindre L, Jiang S, Hwang BJ (1999) J Non-Cryst Solids 255:97
20. Wang JS, Vogel EM, Snitzer E (1994) Opt Mater 3:187
21. Tikhomirov VK, Seddon AB, Furniss D, Ferrari M (2003) J Non-Cryst Solids 326&327:296
22. Ozen G, Demirata B, Ovecoglu ML, Genc A (2001) Spectrochim Acta A 57:273
23. Sun J, Zhang J, Luo Y, Lu S, Ren X, Chen B, Wang X (2006) Opt Mater 28:306
24. Xiao K, Yang Z (2007) Opt Mater 29:1475
25. Babu P, Seo HJ, Kesavulu CR, Jang KH, Jayasankar CK (2009) J Lumin 129:444
26. Yang Y, Yang Z, Chen B, Li P, Li X, Guo Q (2009) J Alloys Compd 479:883
27. Ding Y, Jiang SB, Hwang BC, Luo T, Peyghambarian N, Himei Y, Ito T, Miura Y (2000) Opt Mater 15:123
28. Yang J, Dai S, Zhou Y, Wen L, Hu L, Jiang Z (2003) J Appl Phys 93:977
29. Macfarlane DR, Javorniczky JS, Newman PJ, Booth DJ, Bogdanov V (1995) J Non-Cryst Solids 184:249
30. Azzam RMA, Bashara NM (1977) Ellipsometry and polarized light. North-Holland, Amsterdam
31. Wemple SH (1973) Phys Rev 7:3767
32. Smith DY, Shiles E, Inokuti M (2004) Nucl Instrum Math Phys Res B 218:170
33. Butov OV, Golant KM, Tomashuk AL, van Stralen MJN, Breuls AHE (2002) Opt Commun 213:301
34. Wemple SH (1979) Appl Opt 18:31
35. Mott NF, Davis EA (1979) Electronic processes in non-crystalline materials. Clarendon Press, Oxford
36. Davis EA, Mott NF (1970) Philos Mag 22:903
37. Nelson C, Furukawa I, Nelson WB (1983) Mater Res Bull 18:959
38. Mcswain BD, Borrel NF, Gongjen SV (1963) Phys Chem Glasses 4:1
39. Akamine S, Nanba T, Miura Y, Sakida S (2005) In: 9th biennial worldwide congress on refractories, 8–11 November, Orlando, Florida
40. Berthereau A, Fargin E, Villezusanne A, Olazcuaga R, Le Flem G, Ducasse L (1996) J Solid State Chem 126:142
41. Sakida S (2001) J Am Ceram Soc 84:836
42. Hassan MA, Hogarth CA (1988) J Mater Sci 23:2500 doi: 10.1007/BF01111908
43. Skuja L, Kajihara K, Ikuta Y, Hirano M, Hosono H (2004) J Non-Cryst Solids 345–346:328
44. Dayanand C, Bhikshamaiah G, Salagram M (1995) Mater Lett 23:309
45. Chopra KL, Bahl SK (1972) Thin Solid Films 11:377
46. Subrahmanyam K, Salagram M (2000) Opt Mater 15:181